Modeling the Collective Behavior of Ants on Uneven Terrain

Phi Sigma Undergraduate Research Symposium

Matthew Moreno[1], Dr. Jason Graham[2], Dr. Simon Garnier[3]

April 1st, 2017

[1]University of Puget Sound

[2]University of Scranton

[3]New Jersey Institute of Technology

Mathematical Biosciences Institute

Introduction

Motivation

Figure 1: Ant traffic
[Alexander Wild, a]

Figure 2: Human traffic
[Patrick T. Fallon, 2015]

Background

Figure 3: *Tetramorium caespitum* [Alexander Wild, c]

The collective foraging behavior of ants is well studied, including

- the strategies ants use to engage in foraging behavior [Camazine, 2003]
- how ants tend to select the shortest path to food [Camazine, 2003]
- how ants tend to select the richest food source [Camazine, 2003]
- approaches to mathematical modeling of ant foraging [Perna et al., 2012, Ryan, 2016]

Research Question

- **How does terrain affect the foraging path chosen by ants?**
- To travel between nest to food, do ants tend to select
  - the shortest path,
  - the quickest path,
  - some compromise between these, or
  - some other path all together?
- How might individual ant behaviors on uneven terrain contribute to collective decision making?

Figure 4: *Tetramorium caespitum* [Alexander Wild, b]

Approach

Experimental Design

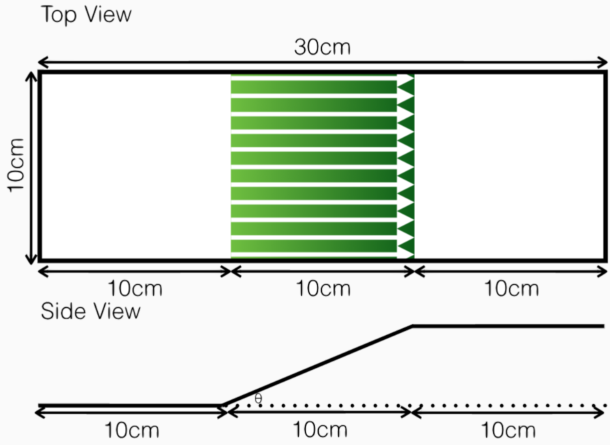

Figure 5: Arena terrain scheme

Modeling Objectives

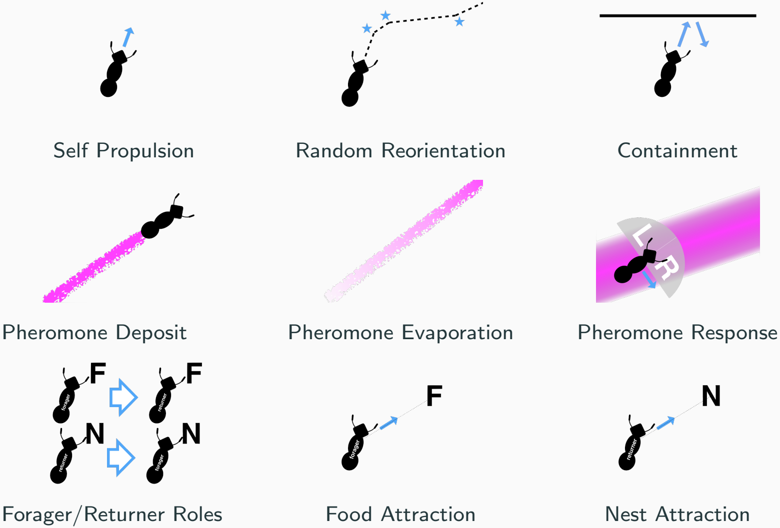

Figure 6: Major modeling considerations

Random Reorientation Events [Khuong et al., 2013]

$$\frac{d}{dt}\begin{pmatrix}\vec{x}\\ \vec{v}\\ s\end{pmatrix} = \begin{pmatrix}\cdots\\ \cdots\\ \|v\|\end{pmatrix}$$

$$\theta_{\text{new}} = \theta_{\text{old}} + \boldsymbol{T}$$
$$s = 0$$
$$s_{\text{thresh}} = \boldsymbol{X}$$

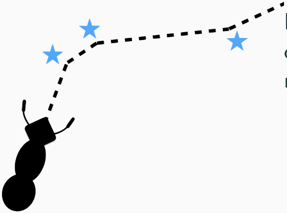

Figure 7: "Boltzmann walker" cartoon; blue stars denote random reorientation events

- upon reaching a threshold distance ($s > s_{\text{thresh}}$), the ant experiences a "reorientation event"
- the threshold distance is generated from an exponential distribution
- the angle the ant turns through is normally distributed

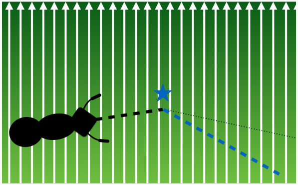

Figure 8: Illustration of adjustment accounting for ant behavior on uneven terrain

$$T_{\text{effective}} = T/\beta$$

$$\beta = \begin{cases} \text{forager role} & e^{c_1 p} \\ \text{returner role} & c_2 \end{cases}$$

$$s_{\text{thresh}} = X + c_3 \frac{|\vec{s} \cdot \vec{v}|}{\|\vec{v}\|}$$

- free path of ant (s_{thresh}) increases if ant oriented with or against the gradient [Khuong et al., 2013]
- ants preferentially re-orient themselves to align with or against a surface's topographical gradient [Khuong et al., 2013]
- severity of random reorientation decreased when following pheromone trail and returning to nest

Complete System

$$\frac{d}{dt}\begin{pmatrix}\vec{x}_1\\ \vec{v}_1\\ s_1\\ \vdots\\ p_1\\ \vdots\end{pmatrix} = \begin{pmatrix} \vec{v}_1 \\ \alpha\hat{\vec{v}}_1\left[\frac{c}{\|\vec{v}\|} - a\|\vec{v}\| + \frac{\|\vec{v}\|^2 - b\vec{v}\cdot\nabla s}{\sqrt{\|\vec{v}\|^2 + (\vec{v}\cdot\nabla s)^2}}\right] + \beta_{\vec{x}}\frac{\vec{a}-\vec{x}_1}{\|\vec{a}-\vec{x}_1\|} + \hat{\vec{v}}_{1\perp}(L_1 - R_1) + \gamma_{\vec{x}}\hat{\vec{v}}_{\perp}\left(\hat{\vec{v}}_{\perp}\cdot\frac{\vec{a}-\vec{x}}{\|\vec{a}-\vec{x}\|}\right) \\ \|\vec{v}_1\| \\ \vdots \\ \kappa f(p_1, \vec{x}_1, \ldots, \vec{x}_n) + \lambda p_1 \\ \vdots \end{pmatrix}$$

events:

- out of bounds $\rightarrow$ reflect heading to "bounce" ant
- $s > s_{\text{thresh}} \rightarrow s = 0$, $s_{\text{thresh}} = \boldsymbol{X} + c_3\frac{|\vec{s}\cdot\vec{v}|}{\|\vec{v}\|}$, random reorientation event with gradient alignment bias
- close to food/nest $\rightarrow$ switch forager/returner role

Animation

Figure 9: Animation of numerically-approximated solution

Results

Results (preliminary): Path Shape

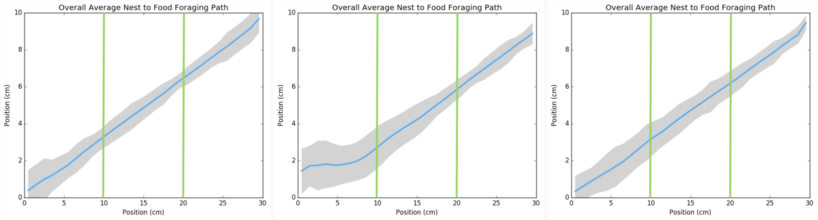

Figure 10: Comparison of overall average nest to food foraging path for, left to right, $-\pi/3$, 0, and $\pi/3$ radian inclines.

Results (preliminary): Path Length

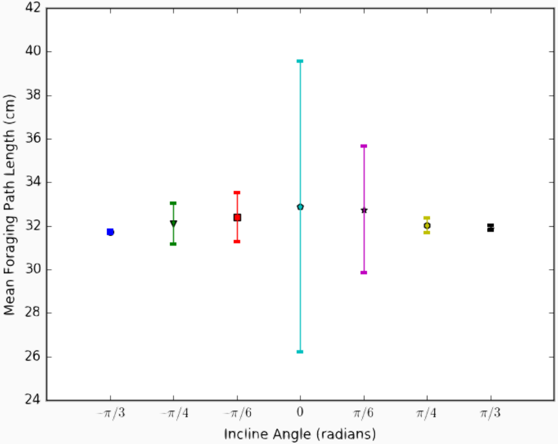

Figure 11: Comparison of path lengths over incline angles for corner-to-corner trials

Next Steps

- Refine model
  - variable pheromone deposition rate
- Perform further sensitivity analyses
  - pheromone grid granularity
  - pheromone sensitivity radius of ant
  - behavioral weighting
- **Compare model predictions with empirical results**

Figure 12: *Tetramorium caespitum* [Alexander Wild, d]

Acknowledgements

- Dr. Garnier and Dr. Graham for their excellent mentorship
- New Jersey Institute of Technology and The Ohio State University
- Mathematical Biosciences Institute (MBI) REU program
- My advisors and mentors at the University of Puget Sound
- This material is based upon work supported by the National Science Foundation under Grant No. 1461163

Questions?

References I

[Alexander Wild, a] Alexander Wild.
ant_battle1-XL.jpg.

[Alexander Wild, b] Alexander Wild.
ant_battle2-XL.jpg.

[Alexander Wild, c] Alexander Wild.
caespitum-16j-XL.jpg.

[Alexander Wild, d] Alexander Wild.
spe2-XL.jpg.

[Camazine, 2003] Camazine, S. (2003).
Self-organization in biological systems.
Princeton studies in complexity. Princeton University Press, Princeton, N.J Woodstock.

References II

[Holt and Askew, 2012] Holt, N. C. and Askew, G. N. (2012).
Locomotion on a slope in leaf-cutter ants: metabolic energy use, behavioural adaptations and the implications for route selection on hilly terrain.
Journal of Experimental Biology, 215(15):2545–2550.

[Khuong et al., 2013] Khuong, A., Lecheval, V., Fournier, R., Blanco, S., Weitz, S., Bezian, J.-J., and Gautrais, J. (2013).
How Do Ants Make Sense of Gravity? A Boltzmann Walker Analysis of Lasius niger Trajectories on Various Inclines.
PLoS ONE, 8(10):e76531.

[Mike Rubenstein, 2014] Mike Rubenstein (2014).
Kilobots31.

[Patrick T. Fallon, 2015] Patrick T. Fallon (2015).
960x0.jpg.

References III

[Perna et al., 2012] Perna, A., Granovskiy, B., Garnier, S., Nicolis, S. C., Labdan, M., Theraulaz, G., Fourcassi, V., and Sumpter, D. J. T. (2012).
Individual Rules for Trail Pattern Formation in Argentine Ants (Linepithema humile).
PLoS Computational Biology, 8(7):e1002592.

[Ryan, 2016] Ryan, S. D. (2016).
A model for collective dynamics in ant raids.
Journal of Mathematical Biology, 72(6):1579–1606.

[SSR Lab, Harvard,] SSR Lab, Harvard.
swarm2.jpg.

Background

Figure 13: Video clip demonstrating route selection by foraging ants

Motivation

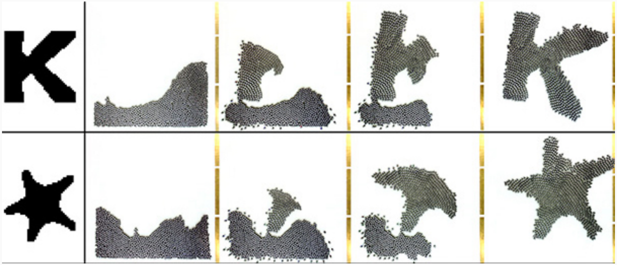

Figure 14: Kilobots in action [Mike Rubenstein, 2014]

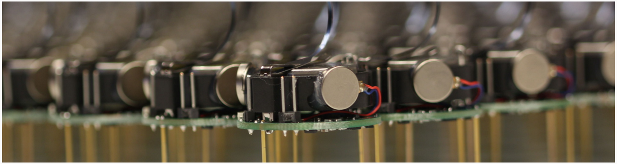

Figure 15: Kilobots, a common swarm robotics platform [SSR Lab, Harvard,]

Background

Figure 16: Video clip of pheromone deposit and response by foraging ants

System of Ordinary Differential Equations: Single Ant

effect of pheromone:

- ant accelerates perpendicular to its orientation
- magnitude of acceleration is proportional to the difference in concentration of pheromone over the “L” and “R” regions

$$\frac{d}{dt}\begin{pmatrix}\vec{x}\\ \vec{v}\end{pmatrix} = \begin{pmatrix}\cdots\\ \hat{\vec{v}}_{\perp}(L-R)\end{pmatrix}$$

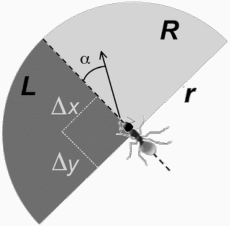

Figure 17: Regions of ant sensitivity to pheromone [Perna et al., 2012]

Results (preliminary): Quickest Center-to-Center Path

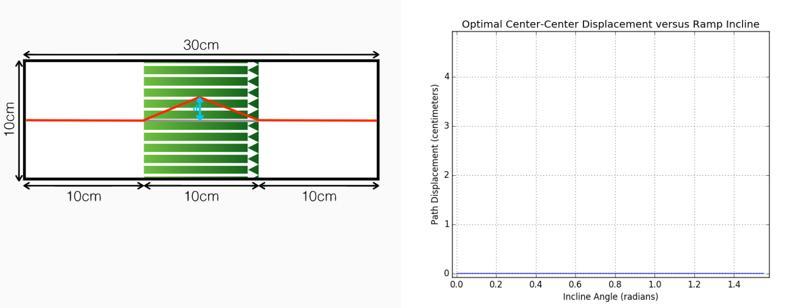

Figure 18: Plot of optimal displacement for quickest center-to-center path with schematic showing displacement.

Results (preliminary): Quickest Corner-to-Corner Path

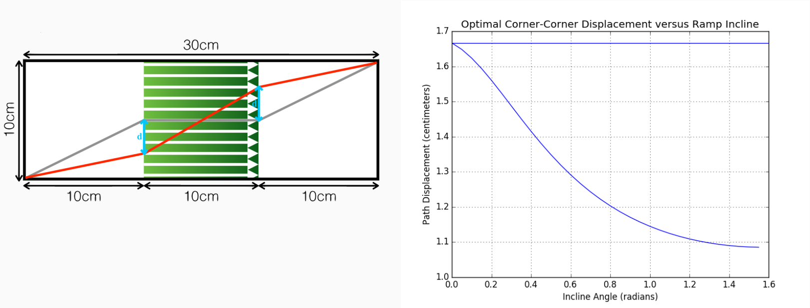

Figure 19: Plot of optimal displacement for quickest corner-to-corner path with schematic showing displacement.

Results (preliminary): Path Shape

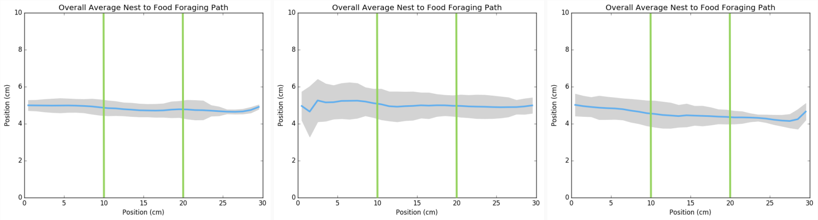

Figure 20: Comparison of overall average nest to food foraging path for, left to right, $-\pi/3$, 0, and $\pi/3$ radian inclines.

Results (preliminary): Path Length

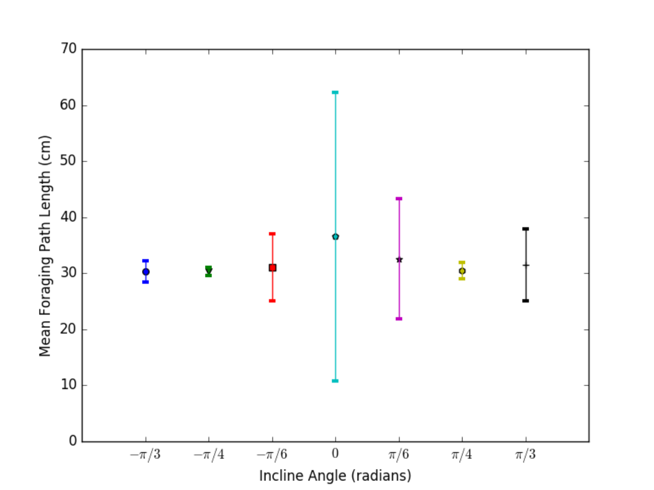

Figure 21: Comparison of path lengths over incline angles for center-to-center trials

Results (preliminary): Path Smoothness

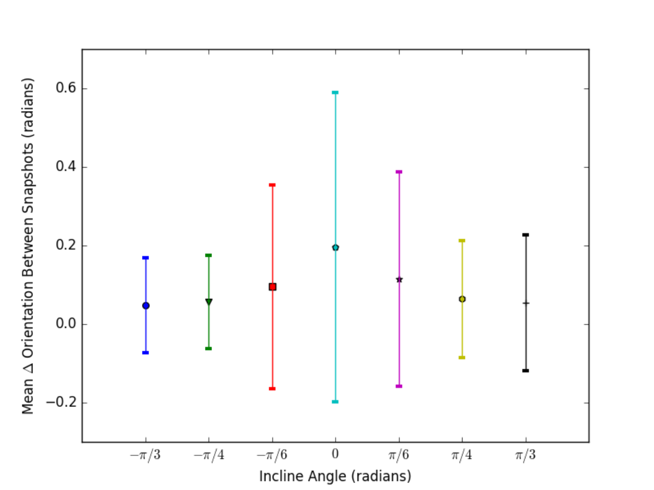

Figure 22: Comparison of changes in heading between shapshots over incline angles for center-to-center trials

Results (preliminary): Trip Duration

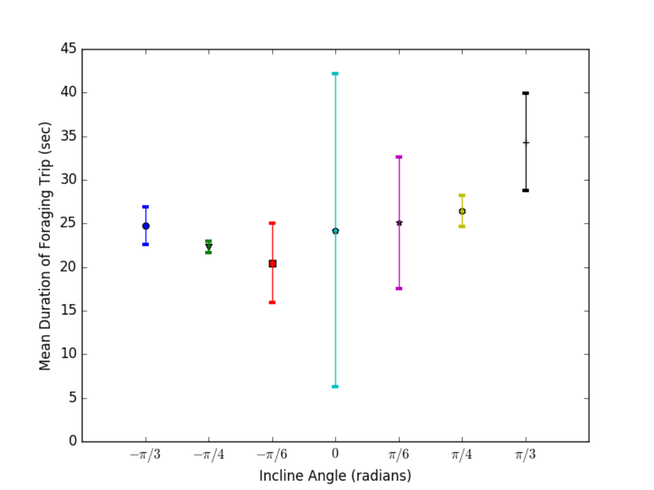

Figure 23: Comparison of trip durations over incline angles for center-to-center trials

Results (preliminary): Orientation Relative to Gradient

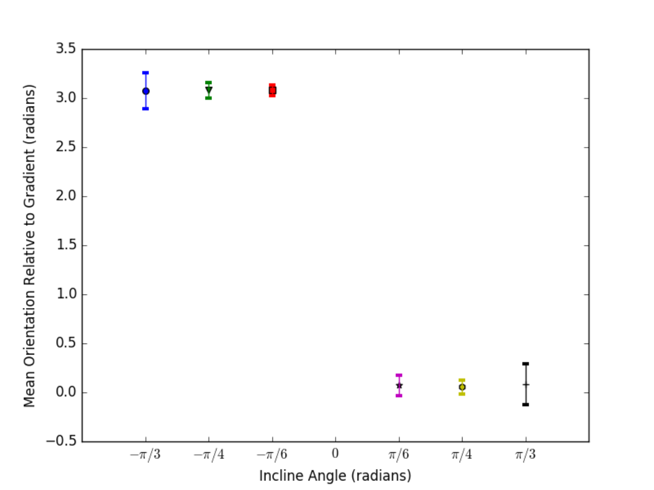

Figure 24: Comparison of orientation relative to gradient over incline angles for center-to-center evaporation rates; the straight path is oriented at 0/3.14 radians

System of Ordinary Differential Equations: Single Ant

$$\frac{d}{dt}\begin{pmatrix}\vec{x}\\ \vec{v}\end{pmatrix} = \begin{pmatrix}\vec{v}\\ \alpha\hat{\vec{v}}(\xi^2 - \|\vec{v}\|^2)\end{pmatrix}$$

self-propulsion: [Ryan, 2016]

- ant accelerates in the direction of its movement if $\|\vec{v}\|\xi$
- ant accelerates against the direction of its movement if $\|\vec{v}\| < \xi$
- "pushes" ant towards a fixed speed
- α is a constant that governs the magnitude of this effect

System of Ordinary Differential Equations: Single Ant

$$\frac{d}{dt}\begin{pmatrix}\vec{x}\\ \vec{v}\end{pmatrix} = \begin{pmatrix}\cdots\\ \beta_{\vec{x}}\frac{\vec{a}-\vec{x}}{\|\vec{a}-\vec{x}\|}\end{pmatrix}$$

attraction to food/nest:

- ant experiences nest attraction if it is in the returner role
- ant experiences food attraction if it is in the forager role
- ant accelerates in the direction of the attractor
- if multiple attractors are present,
  - ant is attracted to nearest food item
  - ant is attracted to midpoint of nest items
- $\beta_{\vec{x}}$ governs the strength of attraction
  - constant for nest attraction
  - for food attraction, decays exponentially with distance from food

System of Ordinary Differential Equations: Single Ant

$$\frac{d}{dt}\begin{pmatrix}\vec{x}\\ \vec{v}\end{pmatrix} = \begin{pmatrix}\cdots\\ \gamma_{\vec{x}}\hat{\vec{v}}_{\perp}\left(\hat{\vec{v}}_{\perp}\cdot\frac{\vec{a}-\vec{x}}{\|\vec{a}-\vec{x}\|}\right)\end{pmatrix}$$

$$\beta = c_1 e^{-c_2\|\vec{a}-\vec{x}\|}$$

near nest attraction:

- ant experiences attraction with magnitude increasing exponentially with proximity to nest
- acceleration is projected onto vector perpendicular to orientation of ant
- ensures that ant goes directly to nest if ant is nearby the nest

System of Ordinary Differential Equations: Pheromone Deposit

$$\frac{d}{dt}p = \kappa f(p, s\vec{x}_1, \ldots, \vec{x}_n)$$

pheromone deposit:

- the rate of pheromone deposit is proportional to total speed of ants located at a tile
- (ants only deposit pheromone when they move)
- let $f(p, \vec{x}_1, \ldots, \vec{x}_n)$ represent a sum of the speeds of of ants associated with the pheromone point p
- κ is a constant governing the magnitude of pheromone deposit

Events

$$t = \begin{cases} 0 & \boldsymbol{U}_1 < \gamma \frac{b_1 - a_1(\cos^2(\phi) - \sin^2(\phi))[c_1 - \hat{\vec{v}} \cdot \hat{\nabla} S]}{\pi/3} \\ 1 & \text{otherwise} \end{cases}$$

$$s = \begin{cases} -1 & \boldsymbol{U}_2 < \frac{\pi - 2d_2 \cos(\phi)[a_2 - 2b_2 \sin(\phi)]}{2\pi} \\ 1 & \text{otherwise} \end{cases}$$

$$\theta_{\text{new}} = \theta_{\text{old}} + \boldsymbol{T},$$
$$\boldsymbol{T} \sim \mathcal{N}(\pi/6 \times g, \sigma^2),$$
$$g = s \times t,$$
$$\boldsymbol{U}_1, \boldsymbol{U}_2 \sim \text{unif}(0, 1)$$

random reorientation events on an incline:

- ant reorientation is biased by $-\pi/6$, 0, or $\pi/6$ radians
- random choices made
  - whether to turn or proceed straight
  - if turning, whether to turn left or right
- probabilities of these choices determined by
  - ϕ, ant orientation relative to gradient
  - γ, angle of inclination

Events

random reorientation events on an incline:

- parameters were fit using Matlab's `lsqcurvefit` and [Khuong et al., 2013]

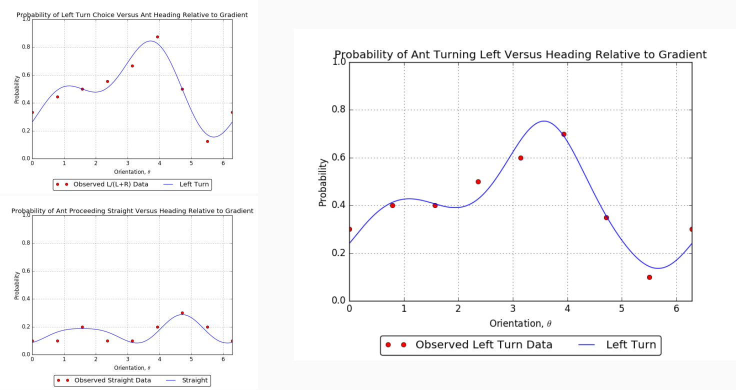

Figure 25: Ant reorientation behavior on an incline ($\gamma = \pi/3$), observed in [Khuong et al., 2013] versus approximated

Numerical Approximation

- deriving an analytic solution is intractable
- take a series of small time steps, using each time point to approximate the next
- Matlab provides a set of ODE solvers that implement sophisticated algorithms for generating numerical solutions to systems of differential equations
- `ode113` was selected to perform simulations

Sensitivity Analysis: Pheromone Evaporation Rate

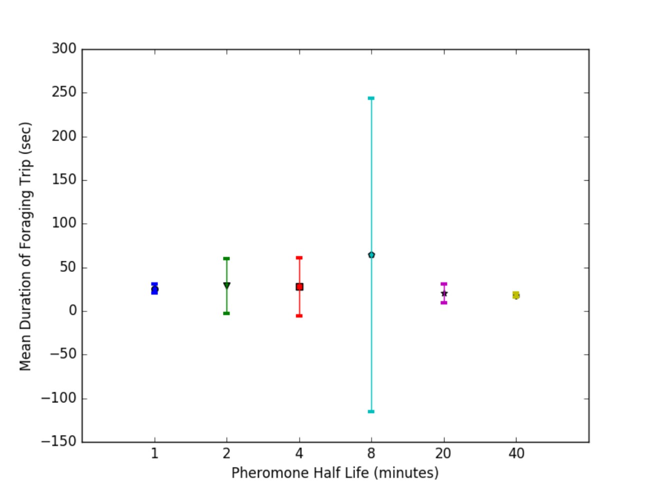

Figure 26: Comparison of durations over pheromone evaporation half lives for center-to-center trials.

Sensitivity Analysis: Pheromone Evaporation Rate

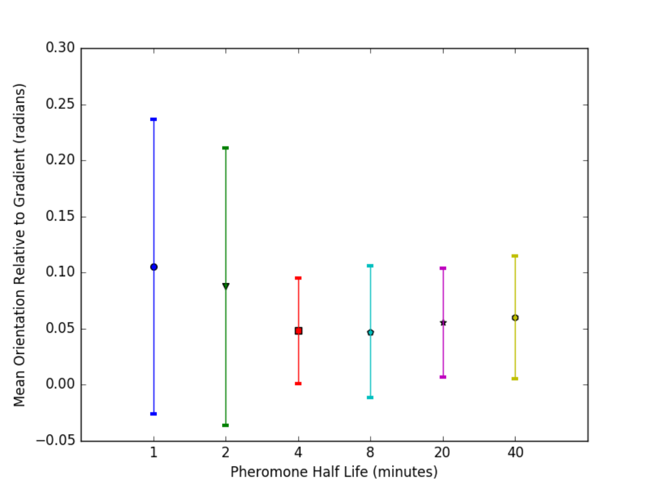

Figure 27: Comparison of orientations relative to gradient over pheromone evaporation half lives for center-to-center trials.

Sensitivity Analysis: Pheromone Evaporation Rate

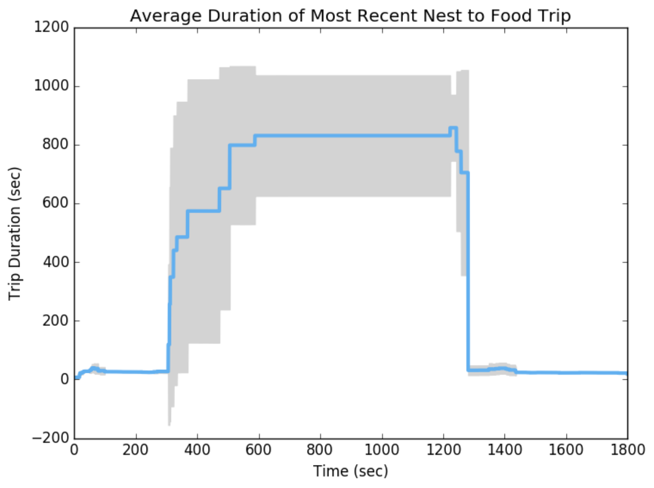

Figure 28: Average trip duration over the course of a 30 minute simulation in a center-to-center arena with 8 minute pheromone half life.

Results (preliminary): Path Shape

Figure 29: Visualization of path as simulation progresses

Results (preliminary): Path Smoothness

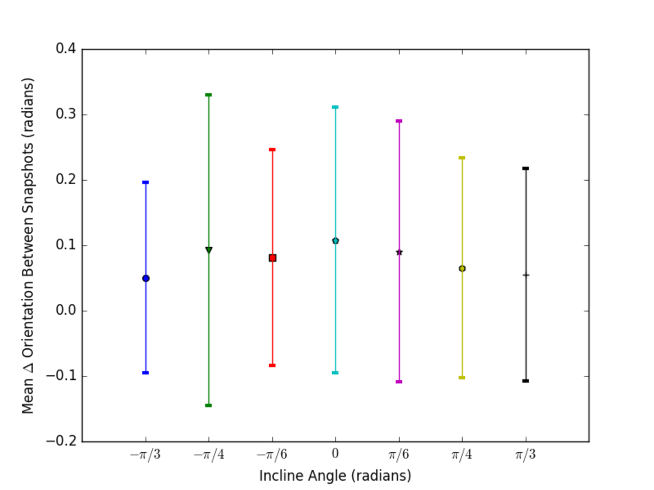

Figure 30: Comparison of changes in heading between shapshots over incline angles for corner-to-corner trials

Results (preliminary): Orientation Relative to Gradient

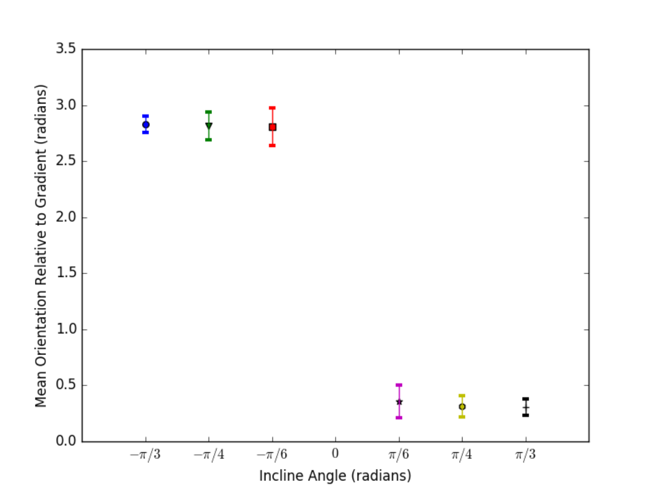

Figure 31: Comparison of orientation relative to gradient over incline angles for corner-to-corner trials; the straight path is oriented at 2.819/0.321 radians

Self Propulsion on Uneven Terrain

$$\frac{d}{dt}\begin{pmatrix}\vec{x}\\ \vec{v}\end{pmatrix} = \begin{pmatrix}\vec{v}\\ \hat{\vec{v}}\left[\frac{c}{\|\vec{v}\|} - a\|\vec{v}\| + \frac{\|\vec{v}\|^2 - b\vec{v}\cdot\nabla s}{\sqrt{\|\vec{v}\|^2 + (\vec{v}\cdot\nabla s)^2}}\right]\end{pmatrix}$$

- ants choose walking speed to expend constant power [Holt and Askew, 2012]
- gravity opposes uphill movement, aids downhill movement
- severe incline/decline decreases overall efficiency of ant movement

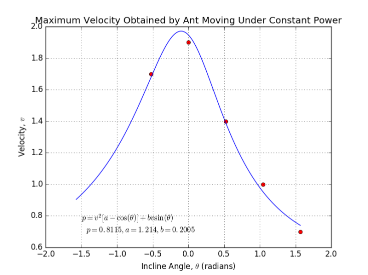

Figure 32: Ant velocity under constant power on inclined terrain

Experimental Design

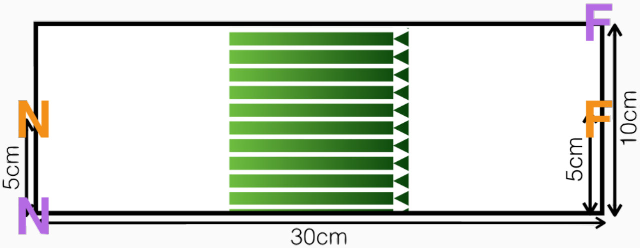

Figure 33: Nest and food placement scheme

Results (preliminary): Trip Duration

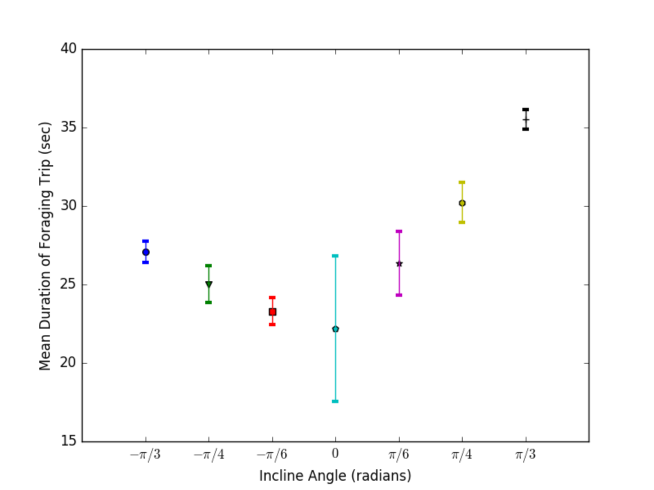

Figure 34: Comparison of trip durations over incline angles for corner-to-corner trials